Structure-Reactivity Relationship in Oxygen and Carbon Monoxide Binding with Some Heme Models

C. Tetreau,*,† D. Lavalette,† M. Momenteau,† J. Fischer,‡ and R. Weiss‡

Contribution from the Institut Curie-Biologie, INSERM U350 and CNRS URA 1387, Centre Universitaire, 91405 Orsay, France, and Institut Le Bel, (URA CNRS-424), Université Louis Pasteur, Strasbourg, 4 rue B. Pascal, 67070 Strasbourg Cedex, France

Received June 20, 1994[⊗]

Abstract: Encumbered heme models have been designed over the years to enforce the Fe-C-O unit to adopt a bent geometry as reported earlier in myoglobin and to examine the consequences upon the reactivity. This work deals with "hybrid" heme models in which a variable amount of distal steric hindrance is provided by a chain which is rigidly maintained in a central position above an iron(II) 5,10,15,20-tetraphenylporphyrin (TPP) macrocycle by the presence of two lateral pivalamido pickets. We have investigated the structure-reactivity relationship in the binding of O_2 and CO with these models by determining the X-ray structures of two CO derivatives and the ligand rebinding kinetics using laser flash photolysis. Upon increasing the steric hindrance, CO affinities are decreased by 2-3 orders of magnitude whereas oxygen affinities are only reduced by a factor of 1.4-3.4, indicating a strong steric discrimination against CO. Using linear free energy relationships to compare all encumbered TPP derivatives for which kinetic data have been reported, we find that a total of six compounds reasonably mimic the reactivity of hemoproteins. The crystal structures of hybrid models as well as other available data indicate that the main mechanisms by which steric interaction with CO is released in encumbered TPP derivatives involve a ruffling distortion of the porphyrin ring and an expansion of the distal cavity instead of the expected bending of the Fe-C-O unit. Many recent experimental and theoretical results suggest that the bent angle of Fe-C-O in myoglobin has been largely overestimated. In fact, several mechanisms may be at work simultaneously to release the steric constraints both in heme models and in hemoproteins, depending on the available degrees of freedom. Although modeling the energetic aspects of hemoprotein reactivity does not imply that structural aspects are also well reproduced, the present results provide additional arguments to reconsider the relative contributions of Fe-C-O and porphyrin distortions for modulating the reactivity in oxygen-carrying hemoproteins.

Introduction

Chemical modeling of oxygen-carrying hemoproteins has markedly contributed to the understanding of the environmental factors governing the reactivity of the active site such as proximal constraints,[1-6] polar distal interactions,[7] and H-bonding of the oxygen ligand.[6,8,9] However, simple unencumbered heme models generally fail to reproduce the relative affinity of hemoproteins for O_2 and CO and bind carbon monoxide with a considerably higher affinity than hemoproteins do. The correlation observed between the vibrational frequency ν_{CO} and the CO affinity in models and hemoproteins,[10] in addition to the available structural data, provided a straightforward explanation for this difference. In agreement with quantum mechanical predictions,[11] the X-ray structure of unconstrained heme models revealed that CO preferentially binds to the Fe^{II} atom in a linear fashion[12] whereas oxygen adopts a bent geometry.[13] In contrast, the Fe-C-O unit was reported to be bent by as much as 120-140° in the CO adduct of sperm whale myoglobin.[14,15] Even more recently, a bent angle of 130-143° was reported in a neutron diffraction study.[16] Accordingly it was widely accepted that the reduced affinity of hemoproteins for CO was a consequence of the bending distortion of the Fe-C-O unit induced by steric interactions of CO with nearby distal amino acid residues.

* To whom correspondence should be addressed. Fax: (33-1) 69 07 53 27. E-mail: laser @ curie.u-psud.fr.

† Centre Universitaire.

‡ Université Louis Pasteur.

⊗ Abstract published in *Advance ACS Abstracts*, November 15, 1994.

(1) Rougee, M.; Brault, D. *Biochemistry* **1975**, *14*, 4100-4106.

(2) Collman, J. P.; Brauman, J. I.; Doxsee, K. M.; Halbert, T. R.; Suslick, K. S. *Proc. Natl. Acad. Sci. U.S.A.* **1978**, *75*, 564-568.

(3) Sharma, V. S.; Geibel, J. F.; Ranney, H. M. *Proc. Natl. Acad. Sci. U.S.A.* **1978**, *75*, 3747-3750.

(4) Geibel, J.; Cannon, J. B.; Campbell, D.; Traylor, T. G. *J. Am. Chem. Soc.* **1978**, *100*, 3575-3585.

(5) White, D. K.; Cannon, J. B.; Traylor, T. G. *J. Am. Chem. Soc.* **1979**, *101*, 2443-2454.

(6) Lavalette, D.; Tetreau, C.; Mispelter, J.; Momenteau, M.; Lhoste, J.-M. *Eur. J. Biochem.* **1984**, *145*, 555-565.

(7) Tetreau, C.; Leondiadis, L.; Lavalette, D.; Momenteau, M. *J. Chem. Soc., Perkin Trans. 2* **1992**, *73*-77.

(8) Lavalette, D.; Tetreau, C.; Momenteau, M.; Mispelter, J.; Lhoste, J.-M.; Wuenschell, G. E.; Reed, C. *Laser Chem.* **1990**, *10*, 297-318.

(9) Wuenschell, G. E.; Tetreau, C.; Lavalette, D.; Reed, C. A. *J. Am. Chem. Soc.* **1992**, *114*, 3346-3355.

(10) Collman, J. P.; Brauman, J. I.; Halbert, T. R.; Suslick, K. S. *Proc. Natl. Acad. Sci. U.S.A.* **1976**, *73*, 3333-3337.

(11) Case, D. A.; Huynh, B. H.; Karplus, M. *J. Am. Chem. Soc.* **1979**, *101*, 4433-4453.

(12) (a) Peng, S.; Ibers, J. A. *J. Am. Chem. Soc.* **1976**, *98*, 8032-8036. (b) Scheidt, W. R.; Kenneth, J. H.; Fons, M.; Mashiko, T.; Reed, C. A. *Biochemistry* **1981**, *20*, 3653-3657.

(13) (a) Collman, J. P.; Gagne, R. R.; Reed, C. A.; Robinson, W. T.; Rodley, G. A. *Proc. Natl. Acad. Sci. U.S.A.* **1974**, *71*, 1326-1329. (b) Jameson, G. B.; Rodley, G. A.; Robinson, W. T.; Gagne, R. R.; Reed, C. A.; Collman, J. P. *Inorg. Chem.* **1978**, *17*, 850-857. (c) Jameson, G. B.; Molinaro, F. S.; Ibers, J. A.; Collman, J. P.; Brauman, J. I.; Rose, E.; Suslick, K. S. *J. Am. Chem. Soc.* **1980**, *102*, 3224-3237.

(14) (a) Cheng, X.; Schoenborn, B. P. *J. Mol. Biol.* **1991**, *220*, 381-399. (b) Cheng, X.; Schoenborn, B. P. *Acta Crystallogr.* **1990**, *B46*, 195-208. (c) Hanson, J. C.; Schoenborn, B. P. *J. Mol. Biol.* **1981**, *153*, 117-146. (d) Norvell, J. C.; Nunes, A. C.; Schoenborn, B. P. *Science* **1975**, *190*, 568-570.

(15) Kuriyan, J.; Wilz, S.; Karplus, M.; Petsko, G. A. *J. Mol. Biol.* **1986**, *192*, 133-154.

(16) Cheng, X.; Schoenborn, B. P. *J. Mol. Biol.* **1991**, *220*, 381-399.

0002-7863/94/1516-11840$04.50/0

To mimic the reactivity of hemoproteins not only toward their natural ligand, oxygen, but also toward the poisonous carbon monoxide ligand has remained a major challenge that has stimulated over the years the search for new models of increasing sophistication. All attempts were focused on the idea to enforce CO to adopt the presumed distorted geometry reported in MbCO and to examine its consequences upon the reactivity. Encumbering groups were anchored either on the meso positions of the porphyrin macrocycle as in the "pocket",[17] "capped",[18] and "hybrid" [19] derivatives of TPP (iron(II) 5,10,15,20-tetraphenylporphyrin) or on the pyrrole rings, as in the "strapped", "cofacial",[20] "cyclophane",[21] "strapped with an aliphatic chain",[22] and "durene-capped" porphyrins.[23] Various amounts of modulation of O_2 and CO affinities have been observed in these families. Extreme examples are the "C_1-cap" which shows no evidence of O_2 and CO binding[24] and a TPP derivative which reversibly binds O_2 but exhibits an unprecedented absence of CO binding.[25]

Laser flash photolysis studies of the CO and O_2 complexes of these sterically hindered porphyrins yielded a wealth of kinetic and thermodynamic information and eventually revealed variable amounts of steric discrimination against CO upon increasing the central steric hindrance. Using linear free energy relationships (LFERs), heme models could be classified into only a small number of families according to their overall reactivity and compared to hemoproteins.[6] However, defining LFER trajectories and connecting reactivity with structure implies that a number of closely related compounds are available for both kinetic and structural investigations.

In this work we report the kinetics and structure of a series of hybrid porphyrins[19] (Figure 1). In these models, a central distal steric hindrance is achieved by an aliphatic chain firmly constrained in a plane perpendicular to the macrocycle by two lateral pivalamido "pickets".

Our data indicate that among TPP derivatives, hybrids **2** and **3** as well as the MedPoc porphyrin[17] mimic the energetic aspects of CO and O_2 binding with hemoproteins reasonably well. In addition we find that steric hindrance does not significantly affect the Fe−C−O bond geometry. The steric constraints are instead mainly released by a pronounced ruffling of the porphyrin macrocycle, a slight doming of the ring toward the proximal ligand, and a large expansion of the distal cavity. A consequence of these motions is that CO can still be accommodated in an almost linear conformation. Similar distortions have been previously reported also for the pocket porphyrin.[26]

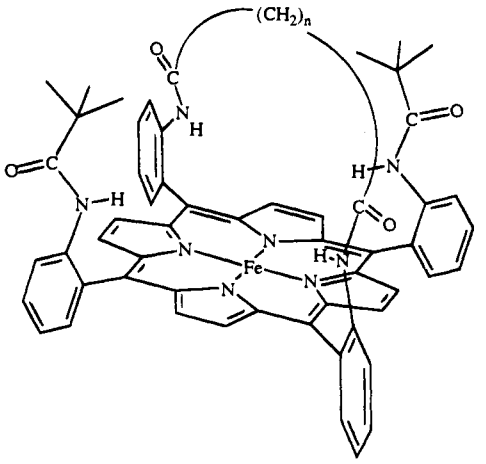

1: n = 10

2: n = 8

3: n = 7

4: n = 6

Figure 1. Formulas of the hybrid models.

At first sight, it might be concluded that there is no univocal structure−reactivity relationship and that modeling the reactivity does not necessarily imply a good modeling of the structural features. One might even suspect that TPP derivatives present excessive flexibility. However, the data upon which the modeling strategy has been currently based have been recently questioned. It has been suggested that the distortion of the Fe−C−O group in proteins might have been largely overestimated, probably because of large experimental uncertainties.[27] Such a severe distortion does not appear consistent with the measured vibrational frequencies of the FeCO group[27,28] nor with calculations which indicate that the energy required for bending the Fe−C−O unit is prohibitive,[27,28] whereas the energy cost for tilting or for porphyrin deformation is far smaller.[29] From a time-resolved polarized infrared absorption study, the Fe−C−O angle was estimated to be 174° and 172° for carboxymyoglobin and carboxyhemoglobin, respectively.[30] A recent X-ray determination of an engineered wild-type MbCO gives an angle of 169°,[31] and a value of 173° has been reported for HbCO.[32]

Although the energetic aspects of hemoprotein reactivity are well reproduced by hybrids **2** and **3**, the main mechanism of steric discrimination against CO involves a distortion of the porphyrin core. These results provide additional arguments to reconsider the relative contributions of Fe−C−O and porphyrin distortions for modulating the reactivity in oxygen-carrying hemoproteins.

Materials and Methods

Materials. The synthesis and characterization of porphyrins **1**−**4** as well as the procedures used for preparing the carboxy- and oxyhemochromes have been described previously.[19] The Fe^{II} forms

(17) Collman, J. P.; Brauman, J. I.; Iverson, B. L.; Sessler, J. L.; Morris, R. M.; Gibson, Q. H. *J. Am. Chem. Soc.* **1983**, *105*, 3052−3064.
(18) Linard, J. E.; Ellis, P. E., Jr.; Budge, J. R.; Jones, R. D.; Basolo, F. *J. Am. Chem. Soc.* **1980**, *102*, 1896−1904.
(19) Momenteau, M.; Loock, B.; Tetreau, C.; Lavalette, D.; Croisy, A.; Schaeffer, C.; Huel, C.; Lhoste, J.-M. *J. Chem. Soc., Perkin Trans. 2* **1987**, 249−257.
(20) Ward, B.; Wang, C.-B.; Chang, C. K. *J. Am. Chem. Soc.* **1981**, *103*, 5236−5238.
(21) (a) Traylor, T. G.; Mitchell, M. J.; Tsuchiya, S.; Campbell, D. H.; Stynes, D. V.; Koga, N. *J. Am. Chem. Soc.* **1981**, *103*, 5234−5236. (b) Traylor, T. G.; Koga, N.; Deardurff, L. A.; Swepston, P. N.; Ibers, J. A. *J. Am. Chem. Soc.* **1984**, *106*, 5132−5143. (c) Traylor, T. G.; Tsuchiya, S.; Campbell, D.; Mitchell, M.; Stynes, D.; Koga, N. *J. Am. Chem. Soc.* **1985**, *107*, 604−614. (d) Traylor, T. G.; Campbell, D. H.; Tsuchiya, S.; Stynes, S.; Mitchell, M. J. In *Hemoglobin and Oxygen Binding*; Ho, C., Ed.; Elsevier, North-Holland: Amsterdam, 1982; pp 425−433.
(22) El-Kasmi, D.; Tetreau, C.; Lavalette, D.; Momenteau, M. *J. Chem. Soc., Perkin Trans. 2* **1993**, 1799−1803.
(23) David, S.; James, B. R.; Dolphin, D.; Traylor, T. G.; Lopez, M. A. *J. Am. Chem. Soc.* **1994**, *116*, 6−14.
(24) Johnson, M. R.; Seok, W. K.; Ibers, J. A. *J. Am. Chem. Soc.* **1991**, *113*, 3998−4000.
(25) Collman, J. P. *J. Am. Chem. Soc.* **1994**, *116*, 2681−2682.
(26) Kim, K.; Fettinger, J.; Sessler, J. L.; Cyr, M.; Hugdahl, J.; Collman, J. P.; Ibers, J. A. *J. Am. Chem. Soc.* **1989**, *111*, 403−404.
(27) Ray, G. B.; Li, X.-Y.; Ibers, J. A.; Sessler, J. L.; Spiro, T. G. *J. Am. Chem. Soc.* **1994**, *116*, 162−176.
(28) Li, X.-Y.; Spiro, T. G. *J. Am. Chem. Soc.* **1988**, *110*, 6024−6033.
(29) Munro, O. Q.; Bradley, J. C.; Hancock, R. D.; Marques, H. M.; Marsicano, F.; Wade, P. W. *J. Am. Chem. Soc.* **1992**, *114*, 7218−7230.
(30) Moore, J. N.; Hansen, P. A.; Hochstrasser, R. M. *Proc. Natl. Acad. Sci. U.S.A* **1988**, *85*, 5062−5066.
(31) Quillin, M. L.; Arduini, R. M.; Olson, J. S.; Phillips, G. N. J. *J. Mol. Biol.* **1993**, *234*, 140−155.
(32) Derewenda, Z.; Dodson, G.; Emsley, P.; Harris, D.; Nagai, K.; Perutz, M.; Reynaud, J.-P. *J. Mol. Biol.* **1990**, *211*, 515−519.

Table 1. Kinetic Rate Parameters and Equilibrium Constants for O_2 and CO Binding with Base Derivatives of Compounds **1**−**4** at 20 °C in Toluene

compound	k_B^{+CO} (M^{-1} s^{-1})	k_B^{-CO} (s^{-1})	K_B^{CO} (M^{-1})	$k_B^{+O_2}$ (M^{-1} s^{-1})	$k_B^{-O_2}$ (s^{-1})	$K_B^{O_2}$ (M^{-1})	M	ref
1−1-MeIm	6.3×10^7	2.7×10^{-3}	2.4×10^{10}	6.2×10^8	1.3×10^2	4.8×10^6	5000	19
1−1,2-Me_2Im	4.7×10^6	$1.1\ 10^{-1}$	4.3×10^7	3.9×10^8	7.5×10^3	5.2×10^4	827	this work
2−1-MeIm	1.8×10^6	2.0×10^{-3}	9.0×10^8	3.0×10^7	2.7×10^1	1.1×10^6	818	19
2−1,2-Me_2Im	1.7×10^5	5.0×10^{-2}	3.4×10^6	1.5×10^7	5.4×10^2	2.8×10^4	121	this work
3−1-MeIm	1.0×10^6	2.6×10^{-3}	3.8×10^8	2.1×10^7	5.0×10^0	4.3×10^6	88	19
3−1,2-Me_2Im	1.0×10^5	3.1×10^{-2}	3.2×10^6	1.0×10^7	6.7×10^1	1.5×10^5	21	this work
4−1-MeIm	8.0×10^4	8.2×10^{-3}	1.0×10^7	2.2×10^6	2.0×10^0	1.4×10^6	7	19
4−1,2-Me_2Im	2.0×10^4	8.0×10^{-2}	2.0×10^5	5.4×10^5	1.5×10^1	3.7×10^4	5.4	this work

were obtained by reduction of Fe^{III} derivatives using sodium dithionite in wet toluene under anaerobic conditions.[33] The hexacoordinated 1,2-Me_2Im−Fe^{II}−CO and 1,2-Me_2Im−Fe^{II}−O_2 complexes were obtained by addition of a known amount of a deaerated 1,2-Me_2Im solution and by bubbling of CO or O_2 through the porphyrin solution. All experiments were performed in toluene *at 20 °C*. Technical details are given in the Experimental Section.

Methods. The bimolecular association rate constants k_B^{+CO} and $k_B^{+O_2}$ and the first-order dissociation rates $k_B^{-O_2}$ (defined according to refs 1 and 5) were obtained from the kinetics of direct or competitive[34] rebinding following photodissociation of the carboxyhemochromes or oxyhemochromes by a laser pulse. All kinetic experiments were performed at 20 °C under pseudo-first-order conditions. Carbon monoxide affinities were obtained from the photometric titration of the carboxyhemochromes against the oxyhemochromes. k_B^{-CO} was obtained as the ratio k_B^{+CO}/K_B^{CO}.

The crystal structures of 1-MeIm−**2**−CO and 1-MeIm−**4**−CO were determined using a single-crystal X-ray diffraction method summarized in the Experimental Section.

Data Evaluation Method: Linear Free Energy Relationships. The tedious and often questionable pairwise comparison of rate parameters and equilibrium constants for a large number of systems is greatly facilitated by plotting log k^+ versus log K. Not only are the changes in rate parameters which are responsible for the change in affinity thus displayed in a simple visual way but the logarithmic representation provides a means to detect the existence of linear free energy relationships (LFERs) upon which a definition and/or classification of reacting families can be rationalized. Previous studies have emphasized the advantage of using LFERs to compare the reactivity of heme models[6,8,22,35] as well as to quantify the changes in reactivity in engineered enzymes.[36] Though it is not new, the method is not so common. For the sake of clarity, we briefly summarize its principles.

Suppose that the representative points of the "on" rates of a number of related compounds undergoing the same reaction happen to fall on a straight line in the log−log plot. Then

$$\log k^+ = \alpha \log K + \log k_o \qquad (1)$$

It follows necessarily that the "off" rates are also linearly correlated according to

$$\log k^- = (\alpha - 1) \log K + \log k_o \qquad (2)$$

It can be easily shown that these relations imply that the free energy changes (δG) of reactants (R), products (P), and transition state (T) upon going from one system to another are not independent but must be related by

$$\delta G_T = \alpha \delta G_P + (1 - \alpha)\delta G_R \qquad (3)$$

As a simple example let us consider the replacement of the proximal ligand in heme models. With respect to this well-defined chemical perturbation the equilibrium constant for binding the sixth ligand is modified due to independent changes of the free energy of both products and reactants. Whenever the linear free energy relationship hypothesis is valid, the change of the free energy of the transition state is not arbitrary but is given by eq 3. The coefficient α measures the amounts of δG_P and δG_R which contribute to δG_T, i.e., the product or reactant character of the transition state. If α is constant within a series of compounds, the representative points of the rate parameters will be aligned in the log−log diagram, defining a "trajectory". Such relations obviously reveal a strong thermodynamic parentage with respect to the chemical or structural perturbation considered. Note that α may not be the same for different perturbations.

When $\alpha = 1$ (purely product-like transition state) or $\alpha = 0$ (purely reactant-like transition state), the changes in affinity are due to changes in only one rate parameter, respectively k^+ and k^-. These particular cases are readily detected in the graphical representation.

Modeling the reactivity of hemoproteins implies that the reactivity of a family of models resembles that of hemoproteins under a similar perturbation. LFERs are particularly useful for performing this global comparison.

Results

Kinetic Study. It has been previously shown that 1-MeIm preferentially binds to the unencumbered face of hybrids **1**−**4**, and that even with the less severely encumbered porphyrins **1** and **2**, hemochromes (1-MeIm−Fe^{II}−1-MeIm) can only be formed at a high base concentration.[19] With 1,2-Me_2Im, binding also occurred preferentially on the free face and hemochrome was not formed, even at the highest concentration used (0.1 M).

The 1,2-Me_2Im−Fe^{II}−O_2 oxyhemochromes of porphyrins **1**−**4** were stable enough toward autooxidation to be studied directly. The carboxy- and oxyhemochromes were found to be photolabile. After laser photodissociation, O_2 (or CO) rebound with the pentacoordinated 1,2-Me_2Im−Fe^{II} complexes according to monoexponential kinetics. In each case, a favorable range of base and gaseous ligand concentrations could be found within which the second-order rate constants were independent of both concentrations, indicating that there was no spoiling of the kinetics by secondary processes such as base elimination or hemochrome formation.[5] The oxygen dissociation rate constants were obtained from the kinetics of competitive rebinding, choosing the base and ligand concentrations for which there was neither base elimination nor hemochrome formation in the direct rebinding experiments. Values of affinity and kinetic rate constants are reported in Table 1; the values previously determined for the 1-MeIm complexes[19] are also given for comparison.

The variations observed upon increasing the amount of steric hindrance from porphyrin **1** to **4** are qualitatively similar for both 1,2-Me_2Im and 1-MeIm complexes; the most striking observation is that the CO affinities are decreased by 2−3 orders of magnitude within the series whereas O_2 affinities are only

(33) Momenteau, M. *Biochim. Biophys. Acta* **1973**, *304*, 814−827.
(34) (a) Noble, R. W.; Gibson, Q. H.; Brunori, M.; Antonini, E.; Wyman, J. *J. Biol. Chem.* **1969**, *244*, 3905−3908. (b) Lavalette, D.; Momenteau, M. *J. Chem. Soc., Perkin Trans. 2* **1982**, 385−388.
(35) Tetreau, C.; Boitrel, B.; Rose, E.; Lavalette, D. *J. Chem. Soc., Chem. Commun.* **1989**, 1805−1806.
(36) Fersht, A. R.; Leatherbarrow, R. J.; Wells, T. N. C. *Biochemistry* **1987**, *26*, 6030−6038.

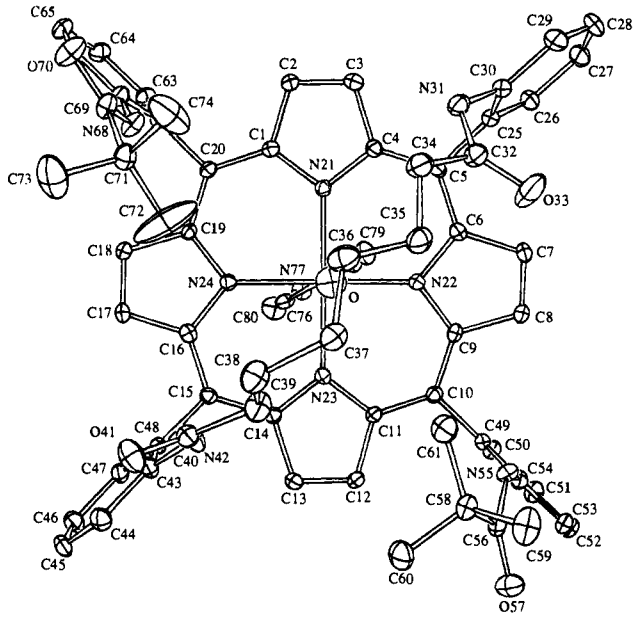

Figure 2. Ortep plot of one molecule of 1-MeIm−**4**−CO showing the numbering scheme used. Ellipsoids are scaled to enclose 50% of the electronic density. Hydrogen atoms are omitted.

reduced by a factor of 1.4−3.4. The strong steric discrimination against CO binding is also reflected in the $M = K_B^{CO}/K_B^{O_2}$ values. Whereas only association rates are decreased for CO, both association and dissociation rates are decreased in a similar proportion for O_2. These findings will be discussed in detail below.

Description of the Structures. The asymmetric units of the crystals of 1-MeIm−**2**−CO·H_2O and 1-MeIm−**4**−CO·1-MeIm contain one porphyrin and one water or 1-MeIm molecule of solvation. The geometry of the 1-MeIm−**4**−CO complex is illustrated in Figure 2 which also gives the numbering scheme used for the atoms. A complete tabulation of the positional and thermal parameters, bond lengths, and bond angles is given in the supplementary material.

In spite of the highly hindered environment, the coordinated CO ligand remains essentially linear, even with porphyrin **4** which has the shortest handle. The Fe−C−O bond angles are, respectively, 178.0(5)° in 1-MeIm−**2**−CO and 178.3(3)° in 1-MeIm−**4**−CO. The Fe−C(CO) and C−O bond distances show the usual values: 1.752(4) and 1.149(6) Å in 1-MeIm−**2**−CO and 1.733(4) and 1.149(5) Å in 1-MeIm−**4**−CO, respectively. Moreover, the Fe−C−O groups are not tilted. The angles between the Fe−C(CO) bonds of 1-MeIm−**2**−CO and 1-MeIm−**4**−CO and the normals to their $4N_p$ mean planes of 1.0(1)° and 1.3(1)°, respectively, are very small.

Both porphyrin cores are slightly domed and substantially ruffled. The doming moves the porphyrinato nitrogens N_p below the porphyrin mean planes away from the encumbering handles. It is indicated by the separations taking place between the $4N_p$ and 24-atom core mean planes which are 0.03(1) and 0.08(1) Å in 1-MeIm−**2**−CO and 1-MeIm−**4**−CO, respectively. The ruffling is indicated by the displacements of the meso carbons relative to the porphyrin core mean planes; the average displacements of these atoms above and below the porphyrin mean planes are 0.29(4) and 0.44(4) Å in 1-MeIm−**2**−CO and 1-MeIm−**4**−CO, respectively. The deviations of the individual atoms from the mean planes of the rings are given in units of 0.01 Å in Figure 3. Negative values indicate atoms displaced away from the porphyrin mean plane toward the proximal side. In spite of significant ruffling, the porphyrinato cores are not strongly buckled. Indeed, the mean of the absolute values of the displacements of the 24 core atoms from their least-squares mean planes does not exceed 0.150(2) and 0.229(2) Å for 1-MeIm−**2**−CO and 1-MeIm−**4**−CO, respectively.

The polymethylene chain forming the handle of **2** is disordered in the crystal structure of 1-MeIm−**2**−CO and adopts two orientations. In these two orientations, the cavity height as measured by the Fe−M distance between the iron atom and the middle (M) of the C36−C37′ or C36−C37″ bonds is 6.809(8) Å. In the 1-MeIm−**4**−CO derivative, the Fe−M distance is only slightly shorter (6.531(5) Å) in spite of the smaller size of the chain. However, these Fe−M vectors are not exactly normal to the $4N_p$ mean planes which also contain the iron atom. In 1-MeIm−**2**−CO and 1-MeIm−**4**−CO, the Fe−M vectors are tipped away from this normal by 1.3(4)° and 2.7(3)°, respectively. Consequently, M is displaced by 0.15(5) Å in 1-MeIm−**2**−CO and 0.31(5) Å in 1-MeIm−**4**−CO from the normal to the $4N_p$ mean plane passing through the iron atom. The shortest distance occurring between the handle and the oxygen atom of carbon monoxide ranges from 3.51(1) Å (C35″) to 3.87(1) Å (C34) in 1-MeIm−**2**−CO and from 3.214(5) Å (C35) to 3.493(7) Å (C39) in 1-MeIm−**4**−CO.

The other structural features of these porphyrin complexes are those expected for hexacoordinate low-spin ferrous derivatives. The mean values of the C−C, C−N, and C−O bond lengths and angles of the porphyrin unit, the two pivalamide pickets, and the 1-MeIm molecule of solvation show the normal expected values. The average Fe−N_p bond distances are 1.991(4) Å in 1-MeIm−**2**−CO and 1.981(3) Å in 1-MeIm−**4**−CO; these values are not significantly different from those found in other hexacoordinate low-spin complexes such as 1-MeIm−**1**−CO, 1.999(2) Å,[37] FeTPP(1-MeIm)$_2$, 1.997(4) Å,[38] FeTPP−CO−Py, 2.03(3) Å,[12] FeDeut−CO−THF, 1.98(3) Å,[12] and FeTPP(Py)$_2$, 1.993(6) Å.[39] The iron atoms lie almost in the $4N_p$ mean planes of the rings, but are slightly displaced from the 24-atom core mean plane toward the 1-methylimidazole ligand (Figure 3).

The axial Fe−N(1-MeIm) bond distances of 2.039(3) and 2.045(2) Å found, respectively, in 1-MeIm−**2**−CO and 1-MeIm−**4**−CO are somewhat longer than those found in the ferrous hexacoordinate low-spin bis(1-MeIm) complex of TPP, especially if one considers the orientation φ of the 1-MeIm mean plane relative to the vectors joining two opposite N_p nitrogens of the porphyrin rings.[40] The orientation angles φ are 32.2(2)° in 1-MeIm−**2**−CO and 35.1(5)° in 1-MeIm−**4**−CO whereas this angle lies close to 10° in FeTPP(1-MeIm)$_2$.[38] The lengthening of the Fe−N(1-MeIm) bond distance could arise from a weak structural trans influence exerted by the CO ligand, leading to a longer axial bond trans to the CO ligand.[41]

As already indicated, the decanediamido handle spanning the ring of porphyrin **2** in 1-MeIm−**2**−CO is disordered and adopts two orientations. In 1-MeIm−**4**−CO, the octanediamidodiphenyl handle spanning the ring of porphyrin **4** displays an unsymmetrical conformation: all the C−C−C−C torsion angles

(37) Ricard, L.; Weiss, R.; Momenteau, M. *J. Chem. Soc., Chem. Commun.* **1986**, 818−820.
(38) Steffen, W. L.; Chun, H.; Hoard, J. L.; Reed, C. A. *Abstracts of Papers*; 175th National Meeting of the American Chemical Society, Anaheim, CA, March 13−17, 1978; American Chemical Society: Washington, DC, 1978.
(39) Li, N.; Petricek, V.; Coppens, P.; Landrum, J. *Acta Crystallogr., C* **1985**, *C41*, 902−905.
(40) Scheidt, W. R.; Haller, K. J.; Fons, M.; Mashiko, T.; Reed, C. A. *Biochemistry* **1981**, *20*, 3653−3657.
(41) Buchler, J. W.; Kokisch, W.; Smith, P. D. *Structure and Bonding*; Springer-Verlag: Berlin, 1978; Vol. 34, pp 79−134.

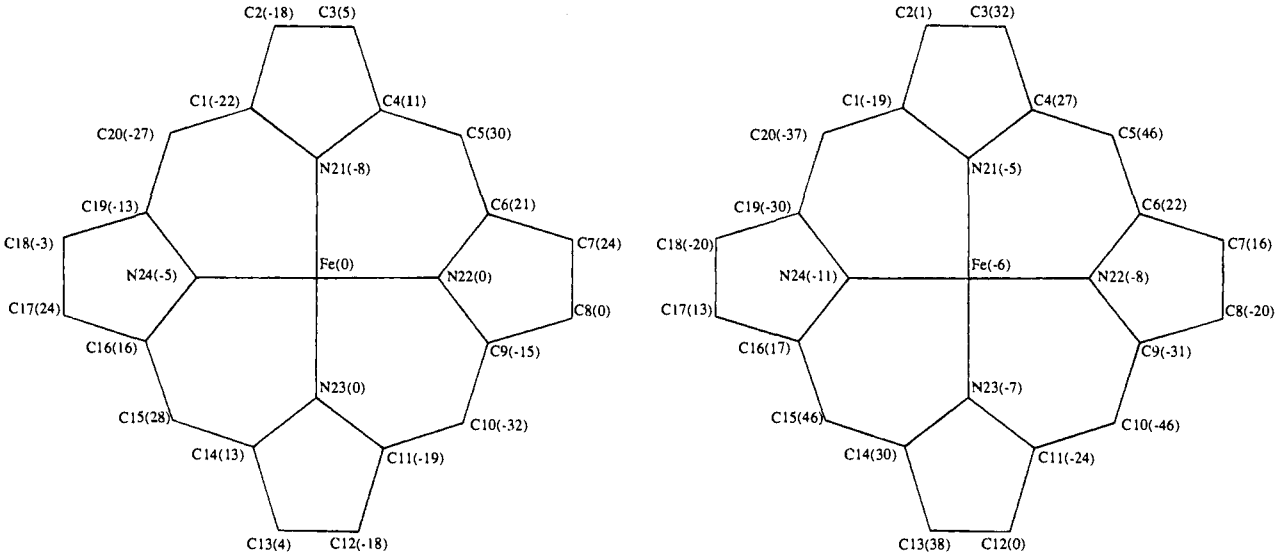

Figure 3. Formal diagram of the porphyrinato core of **2** in 1-MeIm−**2**−CO (a, left) and **4** in 1-MeIm−**4**−CO (b, right). The numbers in parentheses indicate the perpendicular displacement for each atom in units of 0.01 Å from the mean plane of the 24-atom core.

Table 2. Most Significant Structural Features for CO Binding with TPP Derivatives

compound	Fe−C−O (deg)	Fe−M distance (Å)	C_{meso} mean displacement (Å)	shortest NH (amide)−O (CO) distance (Å)	ref
1−(1-MeIm)(CO)	180.0	8.43	0.155		37
2−(1-MeIm)(CO)	178.9	6.81	0.29	4.416	this work
4−(1-MeIm)(CO)	178.3	6.53	0.44	3.989	this work
4−(1-MeIm)		4.56	0.30		42
Fe-β-PocPivP(1,2-Me_2Im)(CO)	172.5		0.53		26
Fe(C_2-cap)(1-MeIm)(CO)					
molecule 1[a]	172.9		0.04		43
molecule 2[a]	175.9		0.03		43

[a] Molecule 1 and molecule 2 are the two Fe(C_2-cap)(1-MeIm)(CO) molecules packed in each crystal unit.

are close to 180° (anti) except two, C36−C37 (−137.6(4)°) and C37−C38 (78.1(5)°).

Discussion

Conformational Reorganization Associated with CO Binding. The most significant structural features are summarized in Table 2, where crystallographic data previously obtained with other hybrid,[37,42] pocket,[26] and capped[43] TPP derivatives are also given for comparison. Increasing the amount of steric hindrance from **1** to **4** has no effect on the Fe−C−O unit which remains essentially linear; however, the ruffling of the porphyrins measured by the mean displacements of the meso carbons relative to the 24-atom core mean planes progressively increases from 0.16 Å in **1** to 0.44 Å in **4**. This progressive distortion is reflected in the optical spectra. The molecular extinction coefficient of the Soret band decreases from 280 to 212 $L{\cdot}mM^{-1}{\cdot}cm^{-1}$ from 1-MeIm−**1**−CO to 1-MeIm−**4**−CO.[19] An accidental distortion due to crystal packing forces or differences in solvation appears therefore unlikely. A comparison of the structures of 1-MeIm−**4** and 1-MeIm−**4**−CO indicates that the mean displacement of the meso carbons which characterize the ruffling of the macrocycles already preexists in the pentacoordinated complex of this highly encumbered porphyrin (0.30 Å) and is increased upon CO ligation (0.44 Å); the increase of ruffling is accompanied by a large expansion of the distal cavity: the chain moves further away from the macrocycle, the cavity height (Fe−M) changing from 4.56 Å in the pentacoordinated species to 6.54 Å in the carboxyhemochrome. From these crystallographic data, we may therefore conclude that the main mechanism by which steric constraints of CO with the handle are released is an expansion of the cavity together with a combined doming and ruffling of the macrocycle. Because such distortions are accompanied by a motion of the handle further away from the iron, CO can still be accomodated in a linear orientation. The data also suggest that the shorter the handle length, the more pronounced this structural reorganization. In spite of the absence of crystallographic data for the 1,2-Me_2Im carbonylated complexes of **1**−**4**, the structural reorganization accompanying CO binding within the series is not expected to differ significantly from that described for 1-MeIm complexes. The absorption spectra of carboxyhemochrome complexes of either base are quite similar, the Soret band of the 1,2-Me_2Im derivatives exhibiting only a 1 nm hyposochromic shift and less than 4% intensity reduction compared to the 1-MeIm complex of the same hybrid. The parallelism in the decrease of the Soret band intensity upon decreasing the chain length as well as the similar decrease of k_B^{+CO} from **1** to **4** with both bases points to a comparable structural reorganization of 1-MeIm and 1,2-Me_2Im complexes.

Although less data are available in the pocket series, the structure of 1,2-Me_2Im−β-PocPiv−CO[26] suggests that the ligand/encumbering group interactions must be released by a similar mechanism, since the Fe−C−O unit is only slightly distorted, whereas the ruffling of the porphyrin is quite substantial (Table 2) and a significant shifting of the benzene "cap" away from the bound carbonyl ligand is also reported in this case.[26] These results appear consistent with recent mo-

(42) Momenteau, M.; Scheidt, W. R.; Eigenbrot, C. W.; Reed, C. A. *J. Am. Chem. Soc.* **1988**, *110*, 1207−1215.
(43) Kim, K.; Ibers, J. A. *J. Am. Chem. Soc.* **1991**, *113*, 6077−6081.

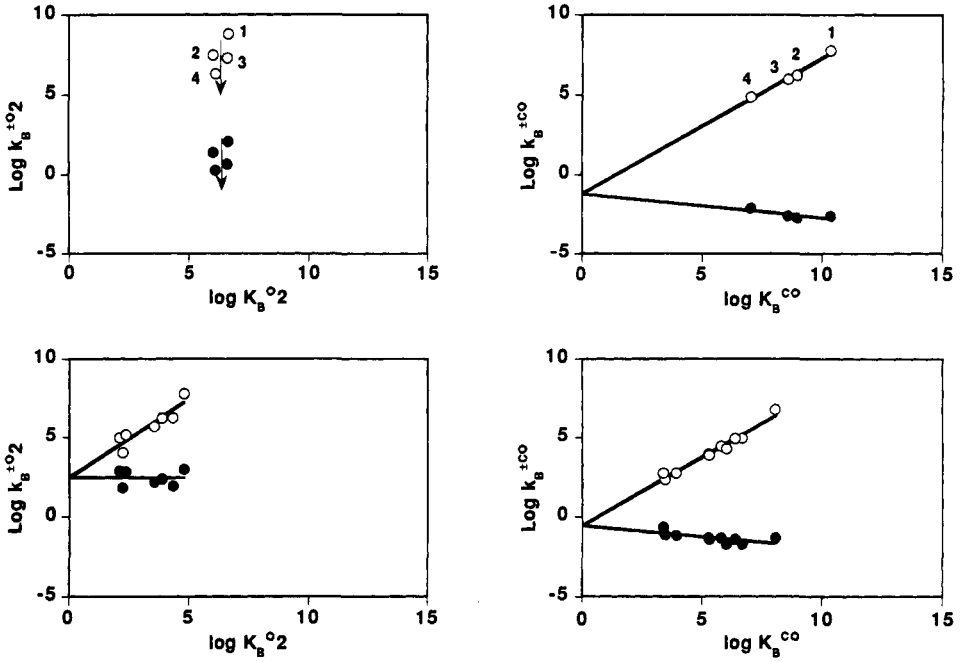

Figure 4. LFERs *obtained at 20 °C* by varying the porphyrin while keeping constant the base (1-MeIm) and the gaseous ligand (oxygen, left, and CO, right): top, hybrid models; bottom, encumbered cyclophane, strapped, and cofacial porphyrins. With the latter porphyrins, 1,5-dicyclohexylimidazole was sometimes used instead of 1-MeIm as a proximal base because the two cyclohexyl substituents prevented binding within the distal cage; however, this base may be considered as quite equivalent to 1-MeIm as concerns its trans influence on O_2 or CO binding properties. Key: open circles, association rates; full circles, dissociation rates. Least-square fits: top, hybrid models; $k_B^{+O_2}$, the lack of continuity in the series **1**−**4** and the narrow range of K^{O_2} values make a linear regression questionable; we consider the trajectories as essentially vertical; k_B^{+CO}, slope = 0.85, intercept = −1.19; k_B^{-CO}, slope = −0.15, intercept = −1.19; bottom, cyclophane, strapped, and cofacial porphyrins; $k_B^{+O_2}$, slope = 1.00, intercept = 2.45; $k_B^{-O_2}$, slope = −0.00, intercept = 2.45; k_B^{+CO}, slope = 0.86, intercept = −0.56; k_B^{-CO}, slope = −0.14, intercept = −0.54.

lecular mechanics calculations suggesting a great flexibility of the porphyrin macrocycle[29] and with experiments indicating that even unstrapped porphyrins may exist in solution as a mixture between planar and ruffled conformations.[44]

In capped carboxyhemochromes, the macrocycle distortion is very small, presumably because the anchorage of the cap on four positions does not allow it; however, a close examination of the structures indicates that CO ligation is accompanied by a large expansion of the cavity while the Fe−C−O unit remains almost linear.[43]

Comparison of Reactivity in Terms of LFERs. As described under Data Evaluation Method, a linear correlation of log k^+ (slope α) and of log k^- (slope $\alpha - 1$) with log K means that the change in free energy at the transition state upon going from one molecule to another is a constant weighted average of the corresponding changes in the free energy of reactants and products. Such relations reveal a strong thermodynamic parentage. Keeping in mind that a LFER and its associated α coefficient are defined with respect to a given chemical or structural perturbation of one of the reactants, we shall first consider in this section the distal steric hindrance as the relevant perturbation and draw the LFER of B−Fe−L complexes obtained by varying the porphyrin while keeping constant the base B and the ligand L. The comparison of the present hybrid models with other sterically encumbered porphyrins is particularly illuminating (Figure 4). In cyclophane,[21] strapped, and cofacial[20] porphyrins, increased steric hindrance manifests itself only in a decrease of association rates for both O_2 and CO. These models are characterized by equal variations of ligand-bound and transition state free energy ($\alpha \approx 1$). In a sense, they do not discriminate between O_2 and CO. In hybrid models, both association and dissociation rates of O_2 are equally affected with a negligible change in affinity. The trajectories connecting the representative points upon going from one hybrid to another in the log $k^{\pm}$ vs log K diagram are almost vertical, showing that the steric interaction manifests itself only in the transition state in oxygen binding. In contrast, the LFER for binding CO with hybrid models is virtually the same as with the other hindered models. In the hybrid series, O_2 and CO are thus distinctly discriminated.

Connection between Reactivity and Structure. Hybrid models have been designed to enforce a permanent central steric hindrance to the binding of distal ligands, the two lateral pickets preventing the encumbering chain from moving sideways. The LFERs (Figure 4) show that hybrid models behave as one homogeneous reacting family. The structures indicate an increased distortion of the porphyrin ring in the series **1**−**4** while the Fe−C−O group remains essentially perpendicular to the mean porphyrin plane. Several recent reports tend to show that distortions of the macrocycle are probably more common than has been thought, even in proteins.[45] Apparently the energetic cost associated with porphyrin distortion accompanying CO binding is much less than the energetic penalty which would

(44) (a) Anderson, K. K.; Hobbs, D. J.; Luo, L.; Stanley, K. D.; Quirke, J. M. E.; Shelnutt, J. A. *J. Am. Chem. Soc.* **1993**, *115*, 12346−12352. (b) Piffat, C.; Melamed, D.; Spiro, T. G. *J. Phys. Chem.* **1993**, *97*, 7441−7450. (c) Sparks, L. D.; Medforth, C. J.; Park, M.-S.; Chamberlain, J. R.; Ondrias, M. R.; Senge, M. O.; Smith, K. M.; Schelnutt, J. A. *J. Am. Chem. Soc.* **1993**, *115*, 581−592. (d) Prendergast, K.; Spiro, T. G. *J. Am. Chem. Soc.* **1992**, *114*, 3793−3801. (e) Shelnutt, J. A.; Medforth, C. J.; Berber, M. D.; Barkigia, K. M.; Smith, K. M. *J. Am. Chem. Soc.* **1991**, *113*, 4077−4087.

(45) (a) Hu, S.; Morris, I. K.; Singh, J. P.; Smith, K. M.; Spiro, T. G. *J. Am. Chem. Soc.* **1993**, *115*, 12446−12458. (b) Louie, G. V.; Brayer, G. D. *J. Mol. Biol.* **1991**, *214*, 527−555. (c) Louie, G. V.; Brayer, G. D. *J. Mol. Biol.* **1990**, *214*, 585−595. (d) Takano, T.; Dickerson, R. E. *J. Mol. Biol.* **1981**, *153*, 79−94. (e) Takano, T.; Dickerson, R. E. *J. Mol. Biol.* **1981**, *153*, 95−115. (f) Deatherage, J. F.; Loe, R. S.; Anderson, C. M.; Moffat, K. *J. Mol. Biol.* **1976**, *104*, 687−706. (g) Takano, T. *J. Mol. Biol.* **1977**, *110*, 537−568.

accompany the bending of the Fe−C−O unit.[27] The LFER of the carboxyhemochromes of **1**−**4** (Figure 4) means that the transition state resembles the ligand-bound state, i.e., that most of the structural rearrangements and energetic characteristics of the product state are already expressed in the transition state for CO binding.

In the absence of the crystallographic structure of the O_2 complexes, we may only speculate about the fact that the steric interaction with the chain which manifests in the transition state is not retained in the "product" state. It does not seem necessary in this case to assume an increase of porphyrin distortion and cavity size upon ligation. The bent orientation of the ligand favors a 4-fold orientational degeneracy in symmetrically substituted hemes. In the "picket fence" [13] as well as in "amide basket handle" porphyrins,[6] the oxygen molecule has been found to point toward the meso positions and eventually undergo some extent of hydrogen bonding with the amide group. In the bound state of the hybrids, an orientation of the Fe−O−O group in the plane connecting the free pickets, though admittedly speculative, could easily minimize the steric interactions with the chain lying in a perpendicular plane to the Fe−O−O unit.

Although the structures of the hexacoordinated complexes of the strapped, cofacial, and cyclophane porphyrins are not available, the difference in their LFERs for CO and O_2 binding compared to the hybrids implies that the steric interaction upon ligand binding must be basically different in both series. In the strapped, cofacial, and cyclophane series a rearrangement of the encumbering group prior to binding would explain that the free energy changes are identical in the transition and bound states of both ligands. In agreement with this view, fast kinetic investigations have revealed that cyclophane porphyrins exist as an equilibrium between an "open" and a "closed" conformation and that ligation occurs only in the open form.[23,46]

Comparison with Hemoproteins: Reactivity. Mammalian hemoproteins were previously shown to follow LFERs for O_2 and CO binding[6,47] which differ significantly from those obeyed by simple heme models.[6] To compare proteins and models, we first have to define the kind of perturbation which has to be considered in drawing LFERs. Whereas the perturbation can be chosen freely with the models, it is imposed and, to a large extent, speculative in the proteins. The LFERs of hemoproteins are rather well defined by the kinetic parameters of the R and T forms of hemoglobin.[6] Since it is now generally accepted that the different reactivities of R and T hemoglobin are associated with a structural rearrangement of the proximal histidine, we have tentatively considered the perturbation induced by a change of the nature of the proximal base while keeping constant the porphyrin and its sixth ligand.

Proximal effects can greatly modify the rate parameters without appreciably affecting the character of the transition state.[6] Even the substitution of a thiolate ligand instead of a nitrogenous base as a proximal ligand is of minor importance from this point of view.[22] As a proximal perturbation we used the replacement of 1-MeIm by 1,2-Me_2Im. This substitution has been shown previously to induce a large change in affinity which is favorable for defining LFER trajectories accurately. The LFERs obtained by changing the proximal base are distinct from those considered in the previous sections where the trajectories were defined by the change of the porphyrin using the same proximal base throughout. It turns out that, with respect to proximal perturbations, a series of models indeed generate LFERs which are close to those of hemoproteins. When

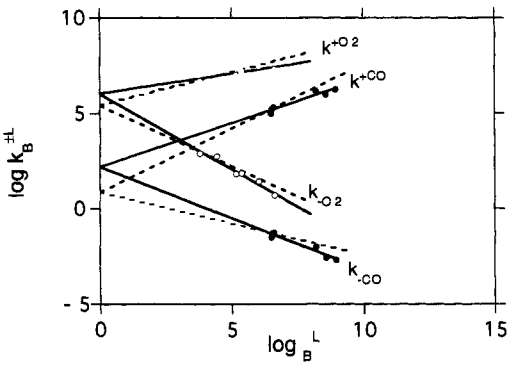

Figure 5. Comparison of the LFERs obtained at 20 °C for CO and O_2 binding with hemoproteins (dotted lines) and models including hybrids **2** and **3** and the MedPoc of ref 17 (full lines). The representative points for the models are given as open circles. Least-square fits: models, $k_B^{+O_2}$, slope = 0.21, intercept = 6.05; $k_B^{-O_2}$, slope = −0.79, intercept = 6.03; k_B^{+CO}, slope = 0.46, intercept = 2.20; k_B^{-CO}, slope = −0.54, intercept = 2.20. Hemoproteins, $k_B^{+O_2}$, slope = 0.35, intercept = 5.43; $k_B^{-O_2}$, slope = −0.64, intercept = 5.43; k_B^{+CO}, slope = 0.67, intercept = 0.86; k_B^{-CO}, slope = −0.33, intercept = 0.87. Error bars are smaller than the size of the symbols.

examining the cloud of points obtained upon plotting the rate parameters of each model liganded successively with 1-MeIm and 1,2-Me_2Im, it was found that, upon changing the proximal base, three models gathered on a single correlation which differs by less than ±0.5 log unit from the correlations for CO or O_2 binding with hemoproteins. As the rate constants are determined within a much greater accuracy, one may assume that all models falling beyond this range cannot be reasonably compared with hemoproteins. The three models define a correlation which includes the 1-MeIm and 1,2-Me_2Im complexes of hybrids **2** and **3** and of "MedPoc" porphyrins, i.e., a total of six points (Figure 5). It is intermediate between that of models with weak "peripheral" steric hindrance (e.g., porphyrin **1** and picket fence and basket handle porphyrins) and that of strongly encumbered compounds (e.g., cyclophane, cofacial, and strapped porphyrins).[6] In spite of some differences, the LFERs obeyed by the "intermediate" models **2**, **3**, and Medpoc are sufficiently close to those of hemoproteins (see Figure 5) to conclude that these compounds, as a whole, reproduce the reactivity of hemoproteins reasonably well.

Comparison with Hemoproteins: Structure. Does energetic modeling imply that structural aspects are also properly reproduced by the heme models? Recent data on porphyrin systems and even on heme proteins lead to the consideration of two complementary aspects of this question: (a) Is the "dogma" of an upright Fe−C−O unit in proteins still acceptable? (b) Is there a unique way for heme models and proteins to release the steric constraints imposed by the ligand geometry?

According to a critical review of the relevant data,[27] it seems that the bent Fe−C−O geometry in hemoproteins is at least questionable. Not only would the reported bent angle of 120−140° imply a prohibitive energy expense, but it also appears to be inconsistent with the recorded Fe−CO vibrational frequencies. Moreover, it is argued that experimental uncertainties do not permit the value of the bent angle to be supported safely. In a very recent high-resolution crystal structure of engineered wild-type MbCO, the Fe−C−O group was found to be nearly linear with a bent angle of 169°.[31] An angle of 173° has been reported for HbCO.[32]

Molecular dynamics calculations[29] and resonance Raman studies have revealed that the porphyrin macrocycle is considerably more flexible than was generally assumed. Simple porphyrins were shown to exist in solution as an equilibrium

(46) Traylor, T. G.; Tsuchiya, S.; Campbell, D.; Mitchell, M.; Stynes, D.; Koga, N. *J. Am. Chem. Soc.* **1985**, *107*, 604−614.
(47) Szabo, A. *Proc. Natl. Acad. Sci. U.S.A.* **1978**, *75*, 2108−2111.

of planar and ruffled conformers.[44] Finally, though not involved in gaseous ligand transport, a regular distortion of the porphyrin from planarity has been observed in a series of seven species of cytochrome *c*.[48]

In comparing our present results with those of hemoproteins, we do not mean that steric constraints are necessarily released by a distortion of the macrocycle in models or in proteins. Doming and ruffling are only one possibility to decrease steric constraints. Structural data are limited in the series of TPP-derived heme models, but in each case where data have been obtained, concerted structural motions have been reported: in "PocPiv", the cap slides away from the Fe−C−O group;[26] in C_2-capped porphyrin, a rearrangement of the cap and its anchoring chains provides a sufficient expansion of the distal pocket to allow a linear accomodation of CO;[43] in hybrids, an increase of the cavity height by about 2 Å is accompanied by a slight off-axis displacement of the chain, in spite of the presence of the lateral pickets.

The possibility that TPP-derived heme models were particularly prone to transfer the steric constraints from the encumbering group to the porphyrin macrocycle has been considered.[21,22] Porphyrins containing a strap anchored on the pyrrole positions have been synthesized and kinetic data collected.[20,21,23,46] It was expected that this mode of anchorage could prevent transfer of the steric constraints because the pyrrole positions were expected to be stiffer than the meso positions. The situation is far from being clear. Several arguments suggest that, in cyclophane models,[20,21,23,46] the macrocycle must remain nearly planar and that, in porphyrins strapped by a methylene chain, The FeCO unit is distorted from linearity.[49,50] The optical absorption spectra of the free bases of porphyrins strapped with a methylene chain become significantly different from that of etioporphyrin only if the chain bears less than 11 CH_2 groups, suggesting that there is a significant deviation from planarity only for a shorter strap.[51] On the basis of the same spectral argument, the 7,7-durene-capped porphyrin is expected to remain essentially planar, whereas the 5,5- and 4,4-durene-capped hemes must exhibit porphyrin distortions.[52] The single available X-ray structure which has been determined within this series concerns the iron(III) chloride derivative of the 4,4-durene-capped porphyrin;[52] the results indicate that the macrocycle is highly distorted. According to molecular mechanics calculations,[29] the energy difference between a "sad" and a "ruf" ruffling deformation is small. Therefore, macrocycles substituted on the meso and pyrrole positions may well have a comparable flexibility.

If it were definitely established that the dogma of a bent Fe−C−O group in proteins must be revised in favor of *an intrinsically upright* geometry, the results of chemical modeling would come into a completely different light. Superstructured porphyrin systems, depending on their particular structure, manage to accomodate the linear CO by undergoing the least expensive distortion. In proteins, a number of additional degrees of freedom are available, as, for instance, in MbCO where the constraints are in part released by a displacement of the distal histidine 64 by 1.4 Å.[27] As previously suggested by others[28] several mechanisms may even be at work concurrently.

(48) Hobbs, J. D.; Anderson, K. K.; Luo, L.; Quirke, J. M. E.; Larsen, R. W.; Shelnutt, J. A. *Biophys. J.* **1994**, *66*, A269.
(49) Gerothanassis, I. P.; Momenteau, M.; Hawkes, G. E.; Barrie, P. J. *J. Am. Chem. Soc.* **1993**, *115*, 9796−9797.
(50) Yu, N.-T.; Kerr, E. A.; Ward, B.; Chang, C. K. *Biochemistry* **1983**, *22*, 4534−4540.
(51) Wijesekera, T. P.; Paine, J. B., III; Dolphin, D.; Einstein, F. W. B.; Jones, T. *J. Am. Chem. Soc.* **1983**, *105*, 6747−6749.
(52) David, S.; James, B. R.; Dolphin, D. *J. Inorg. Biochem.* **1986**, *28*, 125−134.

Conclusions

In this work, we have investigated the structure−reactivity relationship in the binding of O_2 and CO with hybrid models by determining the X-ray structures of two CO derivatives and the ligand rebinding kinetics using laser flash photolysis. Using linear free energy relationships, we find that a total of six encumbered TPP derivatives reasonably mimic the reactivity of hemoproteins. The crystal structures indicate that the main mechanism by which steric interaction with CO is released in encumbered TPP derivatives involves a ruffling distortion of the porphyrin ring and an expansion of the distal cavity, instead of the expected bending of the Fe−C−O unit. Many recent experimental and theoretical results suggest that the bent angle of Fe−C−O in myoglobin has been largely overestimated.

Although modeling the energetic aspects of hemoprotein reactivity does not imply that structural aspects are also well reproduced, the present results provide additional arguments to reconsider the relative contributions of Fe−C−O and macrocycle distortions for modulating the reactivity in oxygen-carrying hemoproteins.

The kinetic and thermodynamic analogies reported here indicate that (i) at least for a number of particular models, the energetic perturbations brought about by steric interactions considered globally are probably similar to those experienced by hemoproteins, (ii) affinity differences among mammalian proteins might result essentially from proximal effects, and (iii) most mammalian hemoglobins probably present, on the average, a similar amount of distal steric hindrance.

Experimental Section

Preparation of Hexacoordinated Complexes of Porphyrins 1−4. The synthesis and characterization of porphyrins **1−4** have been described in ref 19. The Fe^{II} forms were obtained by reduction of Fe^{III} derivatives using sodium dithionite in wet toluene under anaerobic conditions.[33] The pentacoordinated complexes B−Fe^{II} were obtained by addition of a deaerated solution of base, and the carboxy- and oxyhemochromes of porphyrins **1−4** (B−Fe^{II}−CO and B−Fe^{II}−O_2) by further bubbling of CO or O_2 through the solution. The solubilities of oxygen and carbon monoxide in toluene at 20 °C were taken as 7.2 × 10^{-3} and 5.3 × 10^{-3} M·atm^{-1}, respectively.[53]

Kinetic Measurements. The experimental setup was as previously described,[54] except for some modifications performed in order to improve the accuracy. The new Q-switched Nd/Yag laser source ("Quantel") had a pulse width of 10 ns, and its energy could be varied between 1 and 450 mJ at 532 nm. The detection system was as before except for digital recording and in-line data processing. Absorbance changes as small as 10^{-3} can be measured with a time constant of 50 ns. The transient absorption changes were recorded on a Lecroy 9450 digital oscilloscope, and the data were transferred to an Apple MacIntosh II−CI computer via an IEEE-488 interface for conversion of the recorded signals into transient absorbance changes.

The bimolecular association rate constants $k_B{}^{+CO}$ and $k_B{}^{+O_2}$ and the first -order dissociation rates $k_B{}^{-CO}$ and $k_B{}^{-O_2}$ (defined according to refs 1 and 5) were obtained from the kinetics of direct or competitive[34] rebinding following photodissociation of the carboxyhemochromes or oxyhemochromes by a laser pulse. All kinetic experiments were performed under pseudo-first-order conditions. The rate constants have been determined by varying the base concentration over *ca.* 4 orders of magnitude until a range could be found within which the CO and O_2 binding rates remained constant. This procedure has previously been applied[17] to prevent spoiling of the kinetics by various additional processes, such as base elimination or hemochrome formation, which can occur when the base is added as a free ligand in the solution.[5] The following conditions were found to be satisfactory: compounds **1−3**,

(53) Link, W.; Seidell, A. *Solubilities of Inorganic and Metalloorganic Compounds*; Van Nostrand: Princeton, 1958; pp 1236.
(54) Lavalette, D.; Tetreau, C.; Momenteau, M. *J. Am. Chem. Soc.* **1979**, *101*, 5395−5401.

[1,2-Me_2Im] = 0.01−0.1 M, [CO] = 7.2×10^{-4}−7.2×10^{-3} M, [O_2] = 1.0×10^{-3}−5.3×10^{-3} M; compound **4**, [1,2-Me_2Im] = 5×10^{-3}−2×10^{-2} M, [CO] = 7.2×10^{-4}−7.2×10^{-3} M, [O_2] = 1.0×10^{-3}−5.3×10^{-3} M.

Spectrophotometric Titrations. The great stability of the oxygenated complexes of hybrids toward autooxidation allowed the measurement of the partition coefficient $M = K_B^{CO}/K_B^{O_2}$ by photometric titration of the carboxyhemochromes against the oxyhemochromes. The absorbance changes were monitored in the Soret band; measurements were performed at different base concentrations chosen in the range in which kinetic experiments have shown neigher base elimination nor hemochrome formation. The carbon monoxide affinities K_B^{CO} were calculated using M and $K_B^{O_2}$ determined kinetically. The dissociation rate constants k_B^{-CO} were calculated as the ratio k_B^{+CO}/K_B^{CO}.

X-ray Crystal Structure Determination. Suitable single crystals of 1-MeIm−**2**−CO and 1-MeIm−**4**−CO were obtained by slow diffusion of hexane into a toluene solution of porphyrin and base in tubes sealed under CO at room temperature. A systematic search in reciprocal spacing using a Philips PW1100/16 automatic diffractometer showed that crystals of 1-MeIm−**2**−CO·H_2O and 1-MeIm−**4**−CO·MeIm belong to the triclinic and monoclinic systems, respectively. Crystallographic experimental parameters are summarized in Table 3.

Quantitative data were obtained at 173 K using a local-built gas flow device. The resulting data set was transferred to a Vax computer, and for all subsequent calculations the Enraf-Nonius Molen/Vax package[55] was used with the exception of a local data reduction program. Three standard reflections measured every hour during the entire data collection period showed no significant trend. The raw step−scan data were converted to intensities using the Lehmann−Larsen method[56] and then corrected for Lorentz and polarization factors.

Both structures were solved using the heavy atom method. For 1-MeIm−**2**−CO·H_2O, the handle N31−N44 is partially disordered: C34 is linked to C36 over C35′ or C35″, C36 is linked to C38 over C37′ or C37″, and C41 is linked to N44 over C42′/O43′ or C42″/O43″. The occupancies C35′/C35″, C37′/C37″, C42′/C42″, and O43′/O43″ are equal to 0.5/0.5 for the two first and to 0.6/0.4 for the last two as derived from difference peak heights. After refinement of the heavy atoms, difference maps revealed maxima of residual electronic density close to the positions expected for hydrogen atoms. They were introduced in structure factor calculations by their computed coordinates (C−H = N−H = 0.95 Å) and isotropic temperature factors such as $B(H) = 1.3B_{eqv}$ (C or N) Å^2, but not refined. Hydrogen atoms belonging to the handle of 1-MeIm−**2**−CO·H_2O were omitted. At this stage empirical absorption corrections were applied using the method of Walker and Stuart.[57] Full least-squares refinements: $\sigma^2(F^2) = \sigma^2$ counts + $(pI)^2$. A final difference map revealed no significant maxima. The scattering factor coefficients and anomalous dispersion coefficients are from ref 58.

Table 3. X-ray Experimental Parameters

compound	1-MeIm−**2**−CO·H_2O	1-MeIm−**4**−CO·1MeIm
formula	$C_{69}H_{70}N_{10}O_6Fe$	$C_{75}H_{77}N_{14}O_5Fe$
molecular weight	1191.2	1310.4
color	dark blue	dark blue
crystal system	triclinic	monoclinic
a (Å)	13.110(3)	23.394(6)
b (Å)	21.504(6)	11.878(3)
c (Å)	12.009(3)	23.895(6)
α (deg)	99.16(2)	90
β (deg)	111.71(2)	108.84(2)
γ(deg)	81.21(2)	90
U (Å^3)	3089.0	6284.1
Z	2	4
D_{calc} (g cm^{-3})	1.281	1.298
space group	$P\bar{1}$	$P2_1/c$
radiation Cu Kα$_1$ wavelength (Å)	1.5418	1.5418
μ (cm^{-1})	24.280	24.003
crystal size (mm)	0.18 × 0.23 × 0.32	0.13 × 0.18 × 0.22
temperature (K)	173	173
diffractometer	Philips PW1100/16	Philips PW1100/16
scan mode	$\theta/2\theta$ flying step scan	$\theta/2\theta$ flying step scan
scan speed (deg s^{-1})	0.024	0.024
scan width (deg)	0.90 + 0.143 tan(θ)	0.90 + 0.143 tan(θ)
step width (deg)	0.05	0.05
θ limits (deg)	4/57	4/57
octants	±h,±k,+l	±h,±k,+l
number of data points collected	8150	8991
number of data points with $I > 3\sigma(I)$	5906	6024
abs min/max	0.65/1.14	0.90/1.10
$R(F)$	0.063	0.047
$R\omega(F)$	0.086	0.072
p	0.08	0.08
GOF	1.526	1.545

Supplementary Material Available: Tables of positional and thermal parameters, bond lengths, and bond angles for 1-MeIm−**2**−CO·H_2O and 1-MeIm−**4**−CO·1-MeIm (37 pages). This material is contained in many libraries on microfiche, immediately follows this article in the microfilm version of the journal, and can be ordered from the ACS; see any current masthead page for ordering information.

(55) Frenz, B. A. The Enraf-Nonius CAD4-SDP. *Computing in crystallography*; Delft University Press: Delft, The Netherlands, 1978; pp 64−71.

(56) Lehmann, M. S.; Larsen, F. K. *Acta Crystallogr., A* **1974**, *A39*, 580−584.

(57) Walker, N.; Stuart, D. *Acta Crystallogr., A* **1983**, *A39*, 158−166.

(58) Cromer, D. T.; Waber, J. T. *International Tables for X-ray Crystallography*; The Kynoch Press: Birmingham, 1974; Vol. IV.